

Design of large-mode-area multi-core photonic crystal fibers with low confinement loss and dispersion

M. Liu⁺¹⁾, J. Yang*, T. Zhu*

⁺College of Communication Engineering, Chongqing University, 400044 Chongqing, China

*Key Laboratory of Optoelectronic Technology and Systems (Education Ministry of China), Chongqing University, 400044 Chongqing, China

Submitted 3 July 2015

Through doping high refractive index materials into the core region, we propose a kind of large-mode-area multi-core photonic crystal fiber (MCPCF) with low confinement loss and dispersion. The fiber is designed numerically by using full vectorial finite element method (FEM) and the characteristics of the fiber such as effective mode area, confinement loss and dispersion are investigated. The MCPCF exhibits large effective mode area, ultralow confinement loss and dispersion in the communication window of 1–1.6 μm . The MCPCF can be used as matrix fibers in high power fiber lasers with the requirements of high thermal damage threshold and low nonlinear effects.

DOI: 10.7868/S0370274X1517004X

1. Introduction. In recent years, high-power fiber lasers have attracted much attention because of their unique properties such as high beam quality, compactness and high pump frequency [1, 2]. With the obviously intensified power, fiber nonlinearities such as the self-phase modulation, the stimulated Raman and the Brillouin scattering have become the mainly important factors to limit the power scaling of fiber lasers [3].

It's well known that fiber nonlinearities are inversely proportional to the effective mode area and it is an effective approach to reduce the nonlinear effects by increasing the effective mode area [4, 5]. An efficient way is to set the refractive index distribution of PCF reasonably [6–8]. Currently, most of the research on large mode fibers is based on the traditional fiber and single-core PCF [7–10]. However, it's difficult for the traditional fiber to meet the properties such as single-mode transmission, controllable dispersion and loss, as well as large mode area. As for single-core PCFs, it is easy to obtain large mode area by designing flexible structures. Whereas, the problem is that there exists thermomechanical effects for single-core PCFs [11], which implies that the effective mode area cannot be large enough, see 725 μm^2 in Ref. [12].

Comparatively, the multi-core photonic crystal fiber (MCPCF) can provide a flexible structure to realize large mode area and single mode transmission medium [13] which can improve the output power and beam quality [6]. In particular, the thermal stress problems

[14] of the fiber can be solved because of the internal distance between the neighbor cores of MCPCF. In this paper, based on the analysis of different PCF structures, a doped MCPCF is designed to realize large mode area, low confinement loss and dispersion with full vectorial finite element method (FEM) [15, 16].

2. Fiber structure and numerical results. The single-core PCF, four-core PCF and seven-core PCF structures are shown in Fig. 1. The air holes that form the cladding of the fibers have a diameter of $d = 4 \mu\text{m}$, and a pitch $\Lambda = 10 \mu\text{m}$, $d/\Lambda = 0.4$, which implies that light is transmitted in single mode condition [17]. The cores in structures of Figs. 1a, b and d are formed by missing seven air holes, and the cores in the structure of Fig. 1c are formed by missing one air hole. The refractive index of the background is fixed at 1.450 (pure silica).

Effective mode area [18, 19] is one of the most important factors that affect the output power of the fiber laser. It can be controlled effectively by tailoring the core diameter, the number of cores, the cladding air hole pitch size and the index difference between the core and the cladding. The effective mode area can be calculated by the formula [20]:

$$A_{\text{eff}} = \frac{\left(\iint_s |E_t|^2 dx dy \right)^2}{\iint_s |E_t|^4 dx dy} (\mu\text{m}^2), \quad (1)$$

where E is the amplitude of the electric field of the mode.

¹⁾e-mail: liumin@cqu.edu.cn

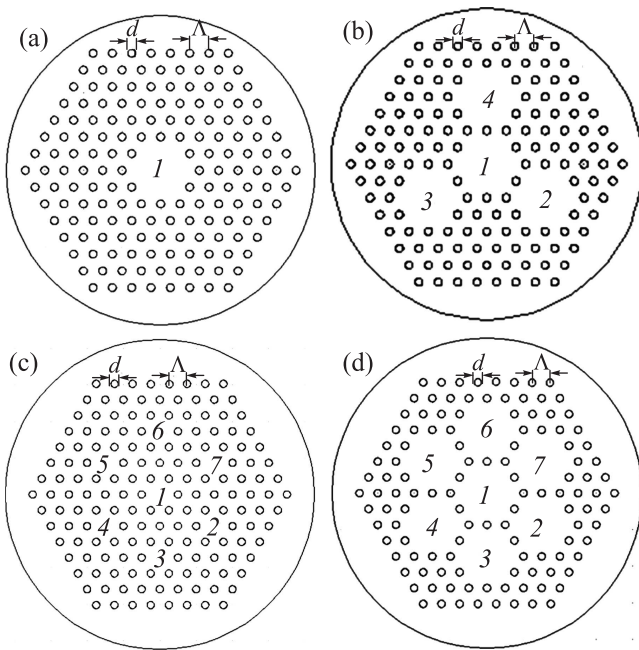


Fig. 1. The cross-section of PCF structure 1 (a), structure 2 (b), structure 3 (c), structure 4 (d)

The wavelength dependence of the effective mode area for the structures of Fig. 1 with $d = 4 \mu\text{m}$ and $\Lambda = 10 \mu\text{m}$ is shown in Fig. 2. It can be seen clearly

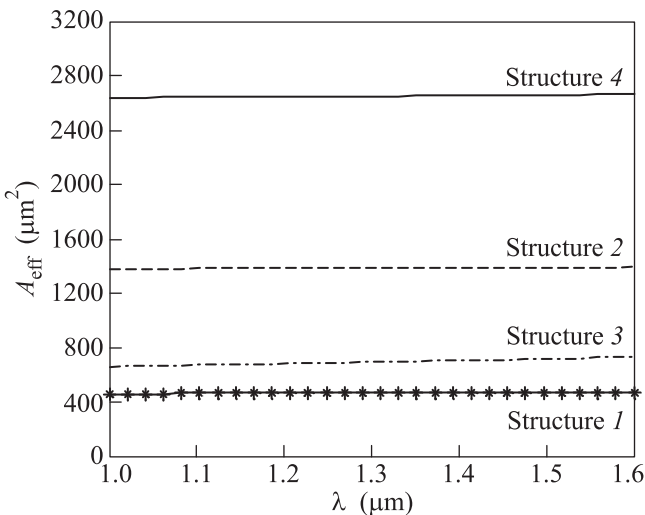


Fig. 2. The effective mode area of PCFs with different structures as a function of wavelength

that the structure 4 has the largest effective mode area ranging from 2640 to 2678 μm^2 while structure 1 has the smallest effective mode area when the wavelength varies from 1.0 to 1.6 μm , which implies that the effective mode area of PCF increases with the number and the area of cores. The variation of the effective mode

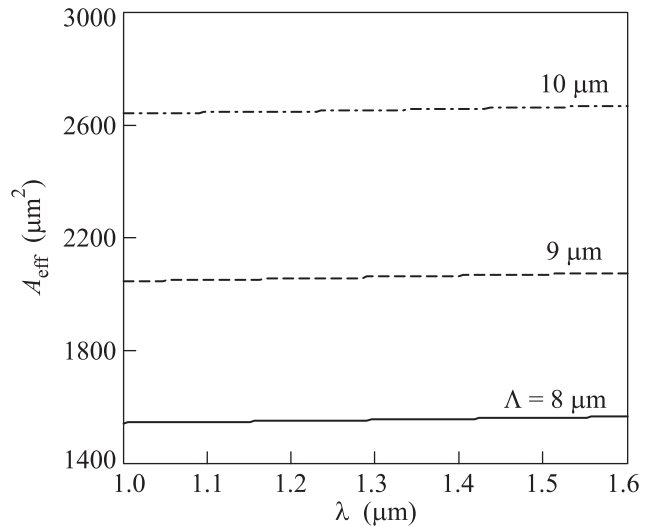


Fig. 3. The effective mode area of PCF with structure 4 as a function of wavelength for different pitch

area with different Λ for structure 4 is shown in Fig. 3. It's indicated that the effective mode area of PCF increases with Λ . In what follows, structure 4 will be used to design large-mode-area MCPCF.

Based on above analysis, a large-mode-area MCPCF is designed as shown in Fig. 4. Each core consists of three

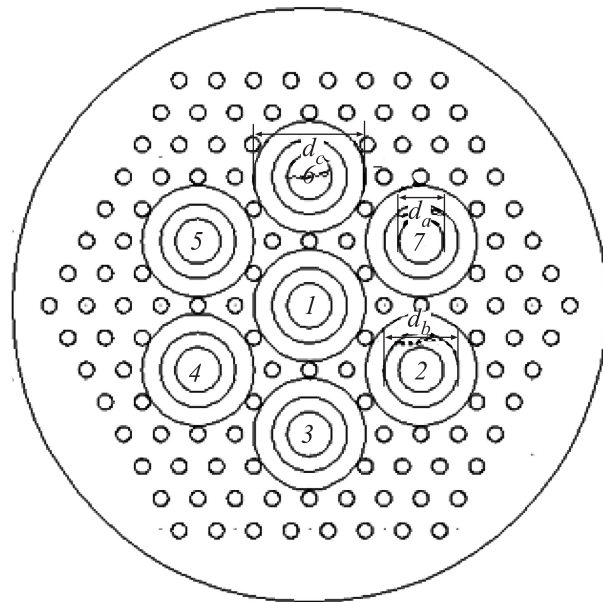


Fig. 4. The cross-section of designed MCPCF

parts: region *a* (pure silica), region *b* (higher-doped refractive index materials) and region *c* (higher-doped refractive index materials). The diameter and the refractive index of the regions are $(d_a, d_b, d_c,)$ and $(n_a, n_b, n_c,)$, respectively.

Table 1. The peak power of PCFs with different structures at $\lambda = 1.31$ and $1.55 \mu\text{m}$

λ	Structure 1	Structure 2	Structure 3	Structure 4	designed MCPCF
$1.31 \mu\text{m}$	$5.206 \cdot 10^{15}$ W/m ²	$2.471 \cdot 10^{15}$ W/m ²	$4.291 \cdot 10^{15}$ W/m ²	$1.336 \cdot 10^{15}$ W/m ²	$9.225 \cdot 10^{14}$ W/m ²
$1.55 \mu\text{m}$	$5.198 \cdot 10^{15}$ W/m ²	$2.455 \cdot 10^{15}$ W/m ²	$4.37 \cdot 10^{15}$ W/m ²	$1.33 \cdot 10^{15}$ W/m ²	$9.407 \cdot 10^{14}$ W/m ²

The mode field distribution of the designed MCPCF with $n_a = 1.450$, $d = 4 \mu\text{m}$, $\Lambda = 10 \mu\text{m}$, $d_a = 8 \mu\text{m}$, $n_b = 1.451$, $d_b = 22 \mu\text{m}$, $n_c = 1.452$, and $d_c = 30 \mu\text{m}$ at $\lambda = 1.31$ and $1.55 \mu\text{m}$ is shown in Figs. 5a and b. We

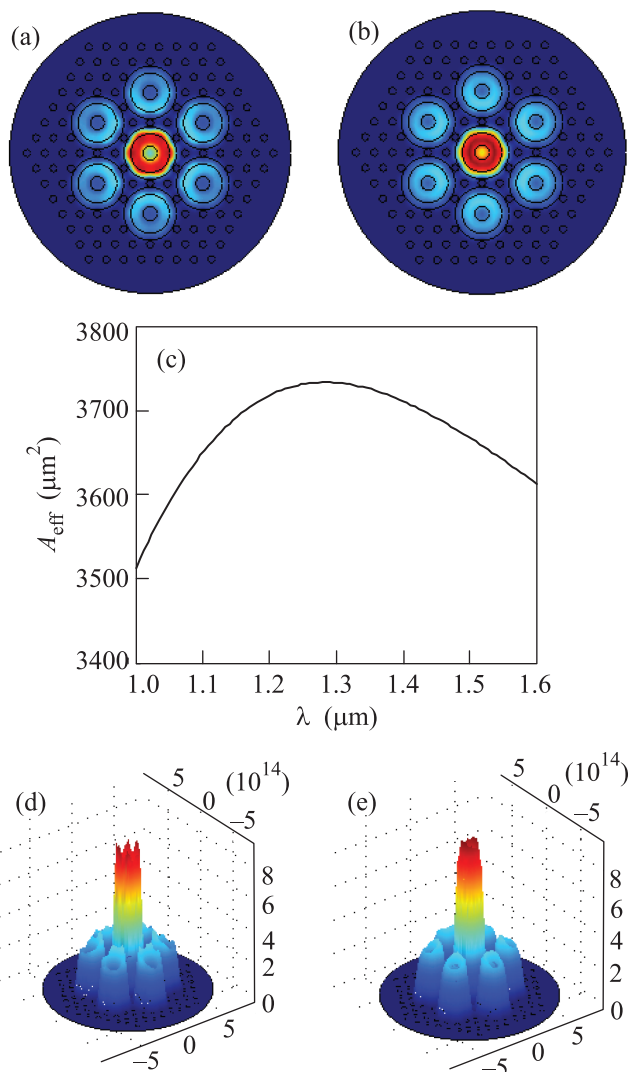


Fig. 5. The properties of designed MCPCF. (a) – The mode field distribution at $\lambda = 1.31 \mu\text{m}$. (b) – The mode field distribution at $\lambda = 1.55 \mu\text{m}$. (c) – The effective mode area as a function of wavelength. (d) – The energy power distribution at $\lambda = 1.31 \mu\text{m}$. (e) – The energy power distribution at $\lambda = 1.55 \mu\text{m}$

can see that the mode field diffuses into region b and region c . The effective mode area of designed MCPCF as a function of wavelength is shown in Fig. 5c. It can be observed that the effective mode area of the designed MCPCF ranges from 3513 to $3733 \mu\text{m}^2$ when the wavelength varies from 1.0 to $1.6 \mu\text{m}$. The effective mode area can be up to $3732 \mu\text{m}^2$ at $\lambda = 1.31 \mu\text{m}$ and $3641 \mu\text{m}^2$ at $\lambda = 1.55 \mu\text{m}$. Figs. 5d and e show the peak power of the PCF at $\lambda = 1.31$ and $1.55 \mu\text{m}$ are $9.225 \cdot 10^{14}$ and $9.407 \cdot 10^{14} \text{ W/m}^2$, respectively. In order to illustrate that the designed MCPCF has low peak power, we compare the peak power of the designed MCPCF with other structures shown in Fig. 1 at $\lambda = 1.31$ and $1.55 \mu\text{m}$ in Table 1. It can be seen that the peak power of MCPCF is the lowest, which means that the designed MCPCF can withstand the highest thermal damage threshold and the lowest nonlinear effects.

It's important to investigate the confinement loss [21] of the designed MCPCF. The confinement loss can be calculated by using the perfectly matched layer (PML) [22] with the formula [21]:

$$L = \frac{2\pi \cdot 8.686 \text{Im}(n_{\text{eff}})}{\lambda} (\text{dB/m}), \quad (2)$$

where $\text{Im}(n_{\text{eff}})$ is the imaginary part of the effective refractive index n_{eff} and λ is the wavelength of light.

The confinement losses of the designed MCPCF with $n_a = 1.450$, $d = 4 \mu\text{m}$, $\Lambda = 10 \mu\text{m}$, $d_a = 8 \mu\text{m}$, $n_b = 1.451$, $d_b = 22 \mu\text{m}$, $n_c = 1.452$, and $d_c = 30 \mu\text{m}$ as a function of wavelength is shown in Fig. 6. We can see that the confinement losses are smaller than 10^{-7} dB/m over the wavelength ranging from 1.0 to $1.6 \mu\text{m}$ and the confinement loss are $5.66 \cdot 10^{-9}$ and $4.27 \cdot 10^{-8} \text{ dB/m}$ at $\lambda = 1.31$ and $1.55 \mu\text{m}$, respectively, which implies very low confinement loss at two common communication wavelengths.

We also analyze the dispersion characteristics of the designed MCPCF, which can be calculated by the formula [23]:

$$D(\lambda) = -\frac{\lambda}{c} \frac{d^2 \text{Re}(n_{\text{eff}})}{d\lambda^2} (\text{ps}/(\text{nm}\cdot\text{km})), \quad (3)$$

where $\text{Re}(n_{\text{eff}})$ is the real part of the effective refractive index n_{eff} , λ is the wavelength of light, and c is the speed of light in a vacuum.

Table 2. The comparison of our designed MCPCF with other reports

Reference design	The effective mode area, μm^2	The confinement loss, dB/m	The dispersion, ps/nm/km
Ref. [8]	2000	\sim	\sim
Ref. [24]	1655	\sim	\sim
Ref. [25]	1070	0.06	1.2
Our MCPCF	3732	$5.66 \cdot 10^{-9}$	-0.502

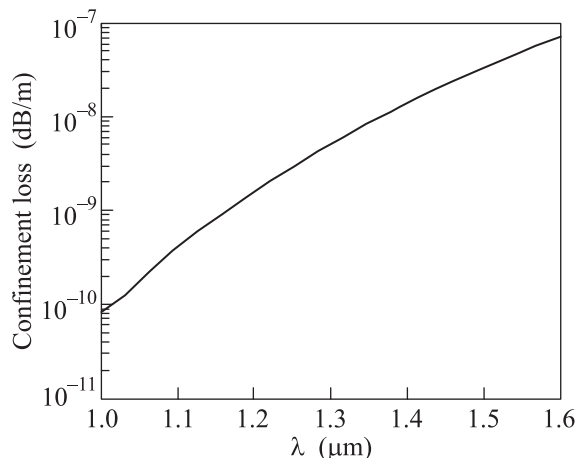


Fig. 6. The confinement loss of designed MCPCF as a function of wavelength

Fig. 7 shows the dispersion of the designed MCPCF with $n_a = 1.450$, $d = 4 \mu\text{m}$, $\Lambda = 10 \mu\text{m}$, $d_a = 8 \mu\text{m}$,

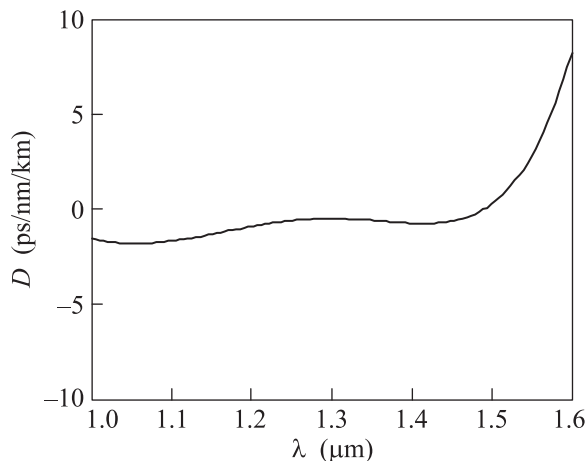


Fig. 7. The dispersion of designed MCPCF as a function of wavelength

$n_b = 1.451$, $d_b = 22 \mu\text{m}$, $n_c = 1.452$, and $d_c = 30 \mu\text{m}$. We can see that the low dispersion can be achieved and the dispersion parameters at $\lambda = 1.31$ and $1.55 \mu\text{m}$ are -0.502 and 2.769 ps/nm/km, respectively, which means the designed MCPCF can achieve anomalous dispersion based on the single mode transmission in the common communication window. It makes it possible to support

the transmission of ultrashort optical pulses, such as optical solitons, which is very important for high power fiber lasers. Meanwhile, no dispersion compensation is needed for our designed MCPCF due to the low dispersion.

In order to illustrate the excellent properties of our designed MCPCF, we compare with other reports [8, 24, 25] from the points of effective mode area, dispersion and confinement loss listed in Table 2. It's easy to find that our designed MCPCF has large effective mode area of $3732 \mu\text{m}^2$, very low confinement loss of 5.66×10^{-9} dB/m and low dispersion of -0.502 ps/nm/km at wavelength $\lambda = 1.31 \mu\text{m}$.

3. Conclusion. We have designed a large effective mode area seven-core PCF by doping the cores with high refractive index materials. It also exhibits ultralow confinement loss and dispersion. The results show that the effective mode area can be up to 3732 and $3641 \mu\text{m}^2$, with the confinement loss of $5.66 \cdot 10^{-9}$ and $4.27 \cdot 10^{-8}$ dB/m, and the dispersion of -0.502 and 2.769 ps/nm/km at $\lambda = 1.31$ and $1.55 \mu\text{m}$, respectively. Our fiber can find potential applications in designing high power fiber laser with good performance.

Project was supported by the Project of Natural Science Foundation of China under Grant # 61475029 and the Fundamental Research Funds for the Central Universities, Project # 106112013CDJZR160006, and 2013 Innovative Team Construction Project of Chongqing Universities (KJTD201331).

1. Q.-Y. Wang, M.-L. Hu, Y.-J. Song, and J. Chinese J. Lasers **34**(12), 1603 (2007).
2. Y.-Y. Yuan and M.-L. Gong, Chinese J. Lasers **35**(9), 1355 (2008).
3. K. Saitoh, T. Muraio, L. Rosa, and M. Koshiha, Opt. Fiber Tech. **16**, 409 (2010).
4. R. K. Varshney, A. K. Ghatak, I. C. Goyal, and S. C. Antony, Opt. Fiber Tech. **9**, 189 (2003).
5. J. K. Dawson, R. J. Beach, and I. Jovanovic, *Conference on Lasers and Electro-Optics/Quantum Electronics and Laser Science Conference*, Technical Digest, Optical Society of America, CWD5 (2003).
6. X. Wang, S.-Q. Lou, and W.-L. Lu, Acta Phys. **62**(18), 184125 (2013).

7. X.-Q. Lu, Q.-L. Zhou, J.-R. Qiu, C.-Sh. Zhu, and D.-Y. Fan *Opt. Comm.* **259**, 636 (2006).
8. Q.-L. Zhou, X.-Q. Lu, and G. Zhang, *Acta Optica Sinica* **30**(5), 1497 (2010).
9. C.-C. Wang, F. Zhang, Y.-C. Lu, R. Geng, and T. Ning, *Opt. Comm.* **282**(11), 2232 (2009).
10. H. Ademgil and S. Haxha, **122**(21), 1950 (2011).
11. C.-Y. Guan, L.-B. Yuan, and J.-H. Shi, *Opt. Comm.* **283**(13), 2686 (2010).
12. M.-Y. Chen, *Optics Express* **15**(19), 12498 (2007).
13. J. C. Knight, T. A. Birks, and P. J. St. Russell, *Opt. Lett.* **21**(19), 1547 (1996).
14. X.-H. Fang, Tian Jin University (2010).
15. B. Rahman, *Progress In Electromagnetics Research* **10**, 187 (1995).
16. S. Guenneu, A. Nicolet, F. Zolla, and S. Lasquellec, *Progress In Electromagnetics Research* **41**, 271 (2003).
17. S. Kim, Ch.-S. Kee, and J. Lee, *J. Optical Society of Korea* **11**(03), 97 (2007).
18. S. Haxha and H. Ademgil, *Opt. Comm.* **281**(2), 278 (2008).
19. N. A. Mortensen, *Opt. Express* **10**(7), 341 (2002).
20. M. Koshihara and K. Saitoh, *Opt. Express* **11**(15), 1746 (2003).
21. H. Ademgil and S. Haxha, *IEEE J. Lightwave Technology* **26**(4), 441 (2008).
22. K. Saitoh, M. Koshihara, T. Hasegawa, and Sasaoka, *Opt. Express* **11**(8), 843 (2003).
23. I. Abdelaziz, F. AbdelMalek, H. Ademgil, Sh. Haxha, T. Gorman, and H. Bouchriha, *J. Lightwave Tech.* **28**(19), 2810 (2010).
24. Y. Zhang, M.-Y. Chen, and J. Zhou, *Acta Phys.* **62**(17), 1742211 (2013).
25. J.-H. Li, J.-Y. Wang, and C. Yan, *Optics Laser Tech.* **48**, 375 (2013).